ultaneously by omitting the primary antibody. Sections were cover slipped using either DPX mountants (Bdh Chemicals) or VectorShield (Vector Laboratories) and analyzed under a Nikon fluorescent microscope equipped with a SPOT camera. All images presented are representative of at least $n = 3-4$ animals examined in each group at each time point.

Morphological analysis

Brain was removed and embedded in paraffin. Mid-sagittal and coronal brain sections (7 μm) were stained with H&E for general pathological observation. Fresh muscle (gastrocnemius and quadriceps) was harvested and flash frozen on 2-methylbutane cooled in liquid nitrogen. Transverse 10 μm sections were processed for H&E, acetylcholinesterase and myosin ATPase (pH 4.3, 4.6 and 9.4) histochemistry according to the standard procedures.

Quantitative assessment of Purkinje cell numbers by BIOQUANT analysis

To estimate the effect of ALS2 inactivation on the number of Purkinje cells, Purkinje cells were counted in age- and region-matched sagittal brain sections from wild-type control and *Als2*-null mice. Half brains were serially sectioned (15 μm) from the midline. The number of Purkinje cells in every 25th sagittal section throughout the entire hemi-cerebellum was determined, as described previously (54,55). The number of Purkinje cells was counted as those identified to be positively immunostained for anti-calbindin antibody along the Purkinje cell layer. Purkinje cell profiles were counted as a function of the length of the Purkinje layer within the same section. Area measurements for Purkinje cell soma were recorded from 100 cells (selected using random sampling methodology) per section counted. All sections were processed simultaneously in an identical manner, and the Purkinje cell counts were performed by the same person (S.C.B.) with the genetic identity of the animals masked, using a light microscope equipped with BIOQUANT Image analysis software (R&M Biometrics).

Motor unit number

MUNE was performed using a modification of the incremental stimulation method (38,41,56). Under inhalation anesthesia, needle stimulation electrodes were inserted close to the sciatic nerve in the proximal leg and threshold for stimulation minimized by small movements of the needle. Recordings were made using a circumferential surface recording electrode around the distal hind limb. A maximum response reflecting activation of all viable motor axons was obtained. Following this, repeated stimuli were applied at very low intensities, slowly increasing the intensity until a single all-or-none response was obtained, reflecting the lowest threshold single motor unit. Intensity was slowly increased until 10 clearly defined increments were obtained, reflecting the summation of the first 10 motor units stimulated. Digital subtraction of successive increments yielded 10 individual motor units; peak-to-peak amplitude was averaged, and this average motor unit amplitude was divided into the peak-to-peak amplitude of the maximum response to yield the MUNE.

Ventral root analysis

The L4 and L5 spinal nerve roots were dissected out and post-fixed in 2% osmium tetroxide in 100 mM cacodylate buffer (pH7.6). After dehydration in graded alcohol, the roots were embedded in Epon (Electron Microscopy Sciences). Semi-thin sections (1 μm) of L4 ventral root were stained with Toluidine blue and examined under light microscope. For quantification, the entire L4 root was imaged and the number of axons, the axon diameter and axon area were marked using Adobe Photoshop software (Version 7.0, Adobe systems) and quantified using Image-J software (Universal Imaging). Individuals performing the analysis were blinded to the mouse genotype. Data are presented as the mean of three mice per group and three counts per root.

Primary culture of neuronal cells

Primary hippocampal cell cultures were established from E18 embryos on a mixed genetic background (F2). In brief, hippocampal tissues were dissected out and immediately placed into 1 ml of ice-cold Hank's Balanced Salts (HBSS)(−) (pH 7.0) (Sigma). After removing HBSS(−) by aspiration, 0.5 ml of 0.25% trypsin–EDTA was added and incubated at 37°C for 15 min. Trypsin–EDTA was removed and washed several times with HBSS(−). Tissue samples were treated with DNase I (final 50 mg/ml) in HBSS(−) at Rtemp for 10 min. The reaction was terminated by adding Dulbecco's modified Eagle's medium (DMEM)/F-12/1:1 (pH7.0) (Invitrogen) containing heat-inactivated 20% (v/v) fetal bovine serum (FBS) (Invitrogen) and incubated at Rtemp for 5 min. After the centrifugation at 150*g* for 15 s, the resulting tissue pellets were dissociated in a 0.6 ml of DMEM/F-12/1:1 (pH 7.0) containing 20% FBS by pipeting using the fire polished Pasteur pipette. After counting the living cell numbers by the Trypan blue assay, the cells were plated onto poly-D-lysine-coated round glasses (BD Biosciences) at an density of 50 cells/mm^2 (low density) or 500 cells/mm^2 (high density) (days *in vivo* 1; DIV1) in neuronal cell culture (NCC) media [DMEM/F-12/1:1 (pH 7.0) containing 1 × B27 supplement (Invitrogen), 25 μM insulin (Sigma), 50 μg/ml streptomycin and 50 U/ml penicillin G] and cultured at 37°C for 12 h. Medium was exchanged with the fresh one containing 5% FBS and cultured for another 36 h. Medium was further replaced with the fresh NCC medium containing both 5% FBS and cytosine-β-D-arabinofuranoside hydrochloride (Ara-C; Sigma), and the cells were cultured until fixation. Finally, cells were fixed with 4% PFA/PBS(−) for 15 min at Rtemp and stained with anti-MAP2 antibody (CHEMICON).

Primary granule cell cultures were established from P6 infants produced by intercrossing the backcrossed (N4) heterozygous mutant mice. The cerebellum tissues were trypsinized and dissociated as above. The dissociated cells were suspended in 4 ml of DMEM/F-12/1:1 (pH 7.0) medium containing 20% (v/v) FBS and plated onto a dish. After incubating at 37°C for 2 h, unattached cells (granule neurons) were recovered from the attached cells (mainly glial cells) on the dish

and centrifuged at 200*g* for 5 min. The resulting pellets were suspended in 1 ml of NCC medium containing 5% FBS, plated onto poly-D-lysine-coated round glasses (BD Biosciences) that were pre-treated with laminin (10 μg/cm^2; Sigma) at a density of 200 cells/mm^2 and cultured for 4 h. The number of sprouting granule cells (axon positive cells/100 cells) was then counted under the light-microscopic observation. Finally, cells were fixed with 4% PFA/PBS(−) for 15 min at Rtemp and stained with anti-βIII tubulin antibody (Tuji-1; Upstate) and Alexa-488 labeled Phalloidin (Molecular probes). Immunofluorescence studies were carried out as previously described (22).

Primary culture of fibroblasts

Primary fibroblast cultures were established from P1 and P2 infants produced by intercrossing the backcrossed (N4) heterozygous mutant mice. The skin tissues were isolated from pups, washed with HBSS(−) and treated with trypsin and DNase I as above. The dissociated cells were seeded onto a T75 flask at an appropriate cell density and cultured in DMEM supplemented with 10% FBS, 100 U/ml penicillin and 100 μg/ml streptomycin.

EGF uptake

Receptor-mediated endocytosis was analyzed by assays for EGF uptake as previously described (22). Briefly, primary fibroblasts were washed with PBS(−) twice and incubated in serum-free medium for 2 h at 37°C, followed by the incubation with serum-free medium containing 800 ng/ml Alexa Fluor-488 labeled EGF (Invitrogen) and 0.1% BSA for 10 min at 37°C. Culture medium was replaced with fresh serum-free medium without ligand and incubated for additional 20 min (total 30 min) or 50 min (total 60 min) at 37°C. Then, the cells were rapidly chilled with ice-cold PBS(−) and fixed with 4% PFA/PBS(−) for 15 min. The cells were washed three times with PBS(−) and permeabilized with 0.1% Triton X-100/PBS(−) at Rtemp for 3 min. Actin fibers of the cells were visualized by the incubation with Alexa Fluor-594 labeled Phalloidin [1:400 with 0.05% Triton X-100/PBS(−); Invitrogen] at Rtemp for 15 min. After washing twice with PBS(−), the cells were mounted with Vectashield with 4′,6-diamidino-2-phenylindole (DAPI) (Vector). Detection and analysis of fluorescent images were conducted by capturing and processing serial optical sections with 0.6–0.8 μm thickness using Leica TCS_NT confocal-microscope systems (Leica Microsystems). For quantitation, randomly selected images were processed to demarcate the outline of each cell, and fluorescent intensities within the demarcated area (corresponding to the single cell) were counted using Leica TCS_NT confocal-microscope systems.

Statistical analyses

Data were analyzed for significance using a Student's *t*-test for pair-wised comparisons or ANOVA followed by Fisher's PLSD *post hoc* test for multiple comparisons between groups (Statview 5.0 software; SAS). Survival data were compared using Kaplan–Meier survival analysis with log-rank test. A *P*-value less than 0.05 was considered as reaching statistical significance.

SUPPLEMENTARY MATERIAL

Supplementary Material is available at HMG Online.

ACKNOWLEDGEMENTS

We thank Ms Yoshiko Yanagisawa, Ms Junko Showguchi-Miyata, Mr Leo Urbinelli, Ms Eri Kohiki and Ms Etsuko Suga for their technical assistance and Dr Kagemasa Kajiwara for generously providing plasmid vectors for the neomycin resistance gene cassette in pKJ2(X) and the diphtheria toxin A gene (DT-A) in pMC1DTpA. This work was funded by the Japan Science and Technology Agency (to J.E.I.) and the Ministry of Health, Labour and Welfare (to J.E.I.). S.H. receives support for a Grant-in-Aid for Scientific Research from the Japan Society of the Promotion of Science, Grant-in-Aid for Scientific Research on Priority Areas—Research on Pathomechanisms of Brain Disorders—(17025039) from MEXT, Takeda Science Foundation and from NOVARTIS Foundation (Japan) for the Promotion of Science. S.C.B. and A.O. are supported by the Muscular Dystrophy Association and a Research Fellowship for Young Scientist from the Japan Society of the Promotion of Science, respectively. R.H.B. receives support for ALS research from the National Institutes of Health (NINDS, NIA), Project ALS, the Angel Fund, the Al-Athel ALS Research Foundation and the Pierre L. deBourghknect ALS Research Foundation.

Conflict of Interest statement. None declared.

REFERENCES

1. Hadano, S., Hand, C.K., Osuga, H., Yanagisawa, Y., Otomo, A., Devon, R.S., Miyamoto, N., Showguchi-Miyata, J., Okada, Y., Singaraja, R. *et al.* (2001) A gene encoding a putative GTPase regulator is mutated in familial amyotrophic lateral sclerosis 2. *Nat. Genet.*, **29**, 166–173.
2. Yang, Y., Hentati, A., Deng, H.X., Dabbagh, O., Sasaki, T., Hirano, M., Hung, W.Y., Ouahchi, K., Yan, J., Azim, A.C. *et al.* (2001) The gene encoding alsin, a protein with three guanine-nucleotide exchange factor domains, is mutated in a form of recessive amyotrophic lateral sclerosis. *Nat. Genet.*, **29**, 160–165.
3. Ben-Hamida, M., Hentati, F. and Ben-Hamida, C. (1990) Hereditary motor system diseases (chronic juvenile amyotrophic lateral sclerosis). *Brain*, **113**, 347–363.
4. Lerman-Sagie, T., Filiano, J., Smith, D.W. and Korson, M. (1996) Infantile onset of hereditary ascending spastic paralysis with bulbar involvement. *J. Child Neurol.*, **11**, 54–57.
5. Eymard-Pierre, E., Lesca, G., Dollet, S., Santorelli, F.M., di Capua, M., Bertini, E. and Boespflug-Tanguy, O. (2002) Infantile-onset ascending hereditary spastic paralysis is associated with mutations in the alsin gene. *Am. J. Hum. Genet.*, **71**, 518–527.
6. Lesca, G., Eymard-Pierre, E., Santorelli, F.M., Cusmai, R., Di Capua, M., Valente, E.M., Attia-Sobol, J., Plauchu, H. Leuzzi, V. Ponzone, A. *et al.* (2003) Infantile ascending hereditary spastic paralysis (IAHSP): clinical features in 11 families. *Neurology*, **60**, 674–682.
7. Devon, R.S., Helm, J.R., Rouleau, G.A., Leitner, Y., Lerman-Sagie, T., Lev, D. and Hayden, M.R. (2003) The first nonsense mutation in alsin results in a homogeneous phenotype of infantile-onset ascending spastic paralysis with bulbar involvement in two siblings. *Clin. Genet.*, **64**, 210–215.

8. Gros-Louis, F., Meijer, I.A., Hand, C.K., Dube, M.P., MacGregor, D.L., Seni, M.H., Devon, R.S., Hayden, M.R., Andermann, F., Andermann, E. *et al.* (2003) An *ALS2* gene mutation causes hereditary spastic paraplegia in a Pakistani kindred. *Ann. Neurol.*, **53**, 144–145.
9. Kress, J.A., Kühnlein, P., Winter, P., Ludolph, A.C., Kassubek, J., Müller, U. and Sperfeld, A.D. (2005) Novel mutation in the *ALS2* gene in juvenile amyotrophic lateral sclerosis. *Ann. Neurol.*, **58**, 800–803.
10. Cleveland, D.W. and Rothstein, J.D. (2001) From Charcot to Lou Gehrig: deciphering selective motor neuron death in ALS. *Nat. Rev. Neurosci.*, **2**, 806–819.
11. Verma, A. and Bradley, W.G. (2001) Atypical motor neuron disease and related motor syndromes. *Semin. Neurol.*, **21**, 177–187.
12. Fink, J.K. (2001) Progressive spastic paraparesis: Hereditary spastic paraplegia and its relation to primary and amyotrophic lateral sclerosis. *Semin. Neurol.*, **21**, 199–207.
13. Kunst, C.B. (2004) Complex genetics of amyotrophic lateral sclerosis. *Am. J. Hum. Genet.*, **75**, 933–947.
14. Ohtsubo, M., Kai, R., Furuno, N., Sekiguchi, T., Sekiguchi, M., Hayashida, H., Kuma, K., Miyata, T., Fukushige, S., Murotsu, T. *et al.* (1987) Isolation and characterization of the active cDNA of the human cell cycle gene (*RCC1*) involved in the regulation of onset of chromosome condensation. *Genes Dev.*, **1**, 585–593.
15. Schmidt, A. and Hall, A. (2002) Guanine nucleotide exchange factors for Rho GTPases: turning on the switch. *Genes Dev.*, **16**, 1587–1609.
16. Burd, C.G., Mustol, P.A., Schu, P.V. and Emr, S.D. (1996) A yeast protein related to a mammalian Ras-binding protein, Vps9p, is required for localization of vacuolar proteins. *Mol. Cell. Biol.*, **16**, 2369–2377.
17. Horiuchi, H., Lippe, R., McBride, H.M., Rubino, M., Woodman, P., Stenmark, H., Rybin, V., Wilm, M., Ashman, K., Mann, M. *et al.* (1997) A novel Rab5 GDP/GTP exchange factor complexed to Rabaptin-5 links nucleotide exchange to effector recruitment and function. *Cell*, **90**, 1149–1159.
18. Tall, G.G., Barbieri, M.A., Stahl, P.D. and Horazdovsky, B.F. (2001) Ras-activated endocytosis is mediated by the Rab5 guanine nucleotide exchange activity of RIN1. *Dev. Cell*, **1**, 73–82.
19. Saito, K., Murai, J., Kajiho, H., Kontani, K., Kurosu, H. and Katada, T. (2002) A novel binding protein composed of homophilic tetramer exhibits unique properties for the small GTPase Rab5. *J. Biol. Chem.*, **277**, 3412–3418.
20. Kajiho, H., Saito, K., Tsujita, K., Kontani, K., Araki, Y., Kurosu, H. and Katada, T. (2003) RIN3: a novel Rab5 GEF interacting with amphiphysin II involved in the early endocytic pathway. *J. Cell Sci.*, **116**, 4159–4168.
21. Sato, M., Sato, K., Fonarev, P., Huang, C.-J., Liou, W. and Grant, B.D. (2005) *Caenorhabditis elegans* RME-6 is a novel regulator of RAB-5 at the clathrin-coated pit. *Nat. Cell Biol.*, **7**, 559–569.
22. Otomo, A., Hadano, S., Okada, T., Mizumura, H., Kunita, R., Nishijima, H., Showguchi-Miyata, J., Yanagisawa, Y., Kohiki, E., Suga, E. *et al.* (2003) ALS2, a novel guanine nucleotide exchange factor for the small GTPase Rab5, is implicated in endosomal dynamics. *Hum. Mol. Genet.*, **12**, 1671–1687.
23. Kunita, R., Otomo, A., Mizumura, H., Suzuki, K., Showguchi-Miyata, J., Yanagisawa, Y., Hadano, S. and Ikeda, J.-E. (2004) Homo-oligomerization of ALS2 through its unique carboxy-terminal region is essential for the ALS2-associated Rab5 guanine nucleotide exchange activity and its regulatory function on endosome trafficking. *J. Biol. Chem.*, **279**, 38626–38635.
24. Yamanaka, K., Vande Velde, C., Eymard-Pierre, E., Bertini, E., Boespflug-Tanguy, O. and Cleveland, D.W. (2003) Unstable mutants in the peripheral endosomal membrane component ALS2 cause early-onset motor neuron disease. *Proc. Natl. Acad. Sci. USA*, **100**, 16041–16046.
25. Topp, J.D., Gray, N.W., Gerard, R.D. and Horazdovsky, B.F. (2004) Alsin is a Rab5 and Rac1 guanine nucleotide exchange factor. *J. Biol. Chem.*, **279**, 24612–24623.
26. Millecamps, S., Gentil, B.J., Gros-Louis, F., Rouleau, G. and Julien, J.P. (2005) Alsin is partially associated with centrosome in human cells. *Biochim. Biophys. Acta.*, **1745**, 84–100.
27. Kanekura, K., Hashimoto, Y., Kita, Y., Sasabe, J., Aiso, S., Nishimoto, I. and Matsuoka, M. (2005) A Rac1/phosphatidylinositol 3-kinase/Akt3 anti-apoptotic pathway, triggered by alsinLF, the product of the *ALS2* gene, antagonizes Cu/Zn-superoxide dismutase (SOD1) mutant-induced motoneuronal cell death. *J. Biol. Chem.*, **280**, 4532–4543.
28. Tudor, E.L., Perkinton, M.S., Schmidt, A., Ackerley, S., Brownlees, J., Jacobsen, N.J.O., Byers, H.L., Ward, M., Hall, A., Leigh, P. N. *et al.* (2005) ALS2/Alsin regulates Rac-PAK signaling and neurite outgrowth. *J. Biol. Chem.*, **280**, 34735–34740.
29. Kanekura, K., Hashimoto, Y., Niikura, T., Aiso, S., Matsuoka, M. and Nishimoto, I. (2004) Alsin, the product of *ALS2* gene, suppresses SOD1 mutant neurotoxicity through RhoGEF domain by interacting with SOD1 mutants. *J. Biol. Chem.*, **279**, 19247–19256.
30. Leavitt, B.R. (2002) Hereditary motor neuron disease caused by mutations in the *ALS2* gene: 'the long and the short of it''. *Clin. Genet.*, **62**, 265–269.
31. Devon, R.S., Schwab, C., Topp, J.D., Orban, P.C., Yang, Y.-Z., Pape, T.D., Helm, J.R., Davidson, T.-L., Rogers, D.A., Gros-Louis, F. *et al.* (2005) Cross-species characterization of the *ALS2* gene and analysis of its pattern of expression in development and adulthood. *Neurobiol. Dis.*, **18**, 243–257.
32. Strausberg, R.L., Feingold, E.A., Grouse, L.H., Derge, J.G., Klausner, R.D., Collins, F.S., Wagner, L., Shenmen, C.M., Schuler, G. D., Altschul, S. F. *et al.* (2002) Generation and initial analysis of more than 15 000 full-length human and mouse cDNA sequences. *Proc. Natl Acad. Sci. USA*, **99**, 16899–16903.
33. Hadano, S., Otomo, A., Suzuki-Utsunomiya, K., Kunita, R., Yanagisawa, Y., Showguchi-Miyata, J., Mizumura, H. and Ikeda, J.-E. (2004) ALS2CL, the novel protein highly homologous to the carboxy-terminal half of ALS2, binds to Rab5 and modulates endosome dynamics. *FEBS Lett.*, **575**, 64–70.
34. Zerial, M. and McBride, H. (2001) Rab proteins as membrane organizers. *Nat. Rev. Mol. Cell Biol.*, **2**, 107–117.
35. Nishimura, T., Fukata, Y., Kato, K., Yamaguchi, T., Matsuura, Y., Kamiguchi, H. and Kaibuchi, K. (2003) CRMP-2 regulates polarized Numb-mediated endocytosis for axon growth. *Nat. Cell Biol.*, **5**, 819–826.
36. Cai, H., Lin, X., Xie, C., Laird, F.M., Lai, C., Wen, H., Chiang, H.-C., Shim, H., Farah, M.H., Hoke, A. *et al.* (2005) Loss of ALS2 function is insufficient to trigger motor neuron degeneration in knock-out mice but predisposes neurons to oxidative stress. *J. Neurosci.*, **25**, 7567–7574.
37. Lipp, H.-P. and Wolfer, D.P. (2003) Genetic background problems in the analysis of congnitive and neuronal changes in genetically modified mice. *Clin. Neurosci. Res.*, **3**, 223–231.
38. Shefner, J.M. (2001) Motor unit number estimation in human neurological diseases and animal models. *Clin. Neurophysiol.*, **112**, 955–964.
39. Fischer, L.R., Culver, D.G., Tennant, P., Davis, A.A., Wang, M., Castellano-Sanchez, A., Khan, J., Polak, M.A. and Glass, J.D. (2004) Amyotrophic lateral sclerosis is a distal axonopathy: evidence in mice and man. *Exp. Neurol.*, **185**, 232–240.
40. Zang, D.W., Lopes, E.C. and Cheema, S.S. (2005) Loss of synaptophysin-positive boutons on lumbar motor neurons innervating the medial gastrocnemius muscle of the $SOD1^{G93A\ G1H}$ transgenic mouse model of ALS. *J. Neurosci. Res.*, **79**, 694–699.
41. Shefner, J.M., Reaume, A.G., Flood, D.G., Scott, R.W., Kowall, N.W., Ferrante, R.J., Siwek, D.F., Upton-Rice, M. and Brown, R.H., Jr (1999) Mice lacking cytosolic copper/zinc superoxide dismutase display a distinctive motor axonopathy. *Neurology*, **53**, 1239–1246.
42. Yang, H.W. and Lemon, R.N. (2003) An electron microscopic examination of the corticospinal projection to the cervical spinal cord in the rat: lack of evidence for cortico-motoneuronal synapses. *Exp. Brain Res.*, **149**, 458–469.
43. Deluca, G.C., Ebers, G.C. and Esiri, M.M. (2004) The extent of axonal loss in the long tracts in hereditary spastic paraplegia. *Neuropathol. Appl. Neurobiol.*, **30**, 576–584.
44. Puls, I., Jonnakuty, C., LaMonte, B.H., Holzbaur, E.L., Tokito, M., Mann, E., Floeter, M.K., Bidus, K., Drayna, D., Oh, S.J. *et al.* (2003) Mutant dynactin in motor neuron disease. *Nat. Genet.*, **33**, 455–456.
45. Münch, C., Sedlmeier, R., Meyer, T., Homberg, V., Sperfeld, A.D., Kurt, A., Prudlo, J., Peraus, G., Hanemann, C.O., Stumm, G. *et al.* (2004) Point mutations of the p150 subunit of dynactin (*DCTN1*) gene in ALS. *Neurology*, **63**, 724–726.
46. Zhao, C., Takita, J., Tanaka, Y., Setou, M., Nakagawa, T., Takeda, S., Yang, H.W., Terada, S., Nakata, T., Takei, Y. *et al.* (2001) Charcot–Marie–Tooth disease type 2A caused by mutation in a microtubule motor KIF1Bb. *Cell*, **105**, 587–597.
47. LaMonte, B.H., Wallace, K.E., Holloway, B.A., Shelly, S.S., Ascano, J., Tokito, M., Van Winkle, T., Howland, D.S. and Holzbaur, E.L. (2002) Disruption of dynein/dynactin inhibits axonal transport in motor neurons causing late-onset progressive degeneration. *Neuron*, **34**, 715–727.

48. Hafezparast, M., Klocke, R., Ruhrberg, C., Marquardt, A., Ahmad-Annuar, A., Bowen, S., Lalli, G., Witherden, A.S., Hummerich, H., Nicholson, S. *et al.* (2003) Mutations in dynein link motor neuron degeneration to defects in retrograde transport. *Science*, **300**, 808–812.
49. Xia, C.-H., Roberts, E.A., Her, L.-S., Liu, X., Williams, D.S., Cleveland, D.W. and Goldstein, L.S.B. (2003) Abnormal neurofilament transport caused by targeted disruption of neuronal kinesin heavy chain KIF5A. *J. Cell Biol.*, **161**, 55–66.
50. Ferreirinha, F., Quattrini, A., Pirozzi, M., Valsecchi, V., Dina, G., Broccoli, V., Auricchio, A., Piemonte, F., Tozzi, G., Gaeta, L. *et al.* (2004) Axonal degeneration in paraplegin-deficient mice is associated with abnormal mitochondria and impairment of axonal transport. *J. Clin. Invest.*, **113**, 231–242.
51. Kieran, D., Hafezparast, M., Bohnert, S., Dick, J.R., Martin, J., Schiavo, G., Fisher, E.M. and Greensmith, L. (2005) A mutation in dynein rescues axonal transport defects and extends the life span of ALS mice. *J. Cell Biol.*, **169**, 561–567.
52. Asano, M., Furukawa, K., Kido, M., Matsumoto, S., Umesaki, Y., Kochibe, N. and Iwakura, Y. (1997) Growth retardation and early death of beta-1,4-galactosyltransferase knockout mice with augmented proliferation and abnormal differentiation of epithelial cells. *EMBO J.*, **16**, 1850–1857.
53. Llewellyn-Smith, I.J., Pilowsky, P. and Minson, J.B. (1992) Retrograde tracers for light and electron microscopy. In Bolam, J.P. (ed.), *Experimental Neuroanatomy: A Practical Approach*. Oxford University Press, New York, pp. 32–59.
54. Duchala, C.S., Shick, H.E., Garcia, J., Deweese, D.M., Sun, X., Stewart, V.J. and Maclin, W.B. (2004) The toppler mouse: a novel mutant exhibiting loss of Purkinje cells. *J. Comp. Neurol.*, **476**, 113–129.
55. Zanjani, H., Lemaigre-Dubreuil, Y., Tillakaratne, N.J., Blokhin, A., McMahon, R.P., Tobin, A.J., Vogel, M.W. and Mariani, J. (2004) Cerebellar Purkinje cell loss in aging Hu-Bcl-2 transgenic mice. *J. Comp. Neurol.*, **475**, 481–492.
56. Shefner, J.M., Jillapalli, D. and Bradshaw, D.Y. (1999) Reducing intersubject variability in motor unit number estimation. *Muscle Nerve*, **22**, 1457–1460.

[26] Purification and Functional Analyses of ALS2 and its Homologue

By Shinji Hadano and Joh-E Ikeda

Abstract

ALS2 is a causative gene product for a form of the familial motor neuron diseases. Computational genomic analysis identified ALS2CL, which is a novel protein highly homologous to the C-terminal region of ALS2. Both proteins contain the VPS9 domain, which is a hallmark for all known members of the guanine nucleotide exchange factors for Rab5 (Rab5GEF), and are known to act as novel factors modulating the Rab5-mediated endosome dynamics in the cells. It has also been reported that oligomerization of ALS2 is one of the fundamental features of its biochemical and physiological function involving endosome dynamics. This chapter describes methods, including purification of the recombinant ALS2 and ALS2CL, and Rab5GEF assay, which have been utilized to clarify the molecular function for ALS2 and ALS2CL.

Introduction

The small GTPases control a broad spectrum of cellular and molecular processes, such as nuclear transfer, cytoskeletal organization, various signaling cascades, and neuronal morphogenesis (Da Silva and Dotti, 2002; Etienne-Manneville and Hall, 2002; Govek *et al.*, 2005; Luo, 2000; Van Aelst and Symons, 2002). All of the small GTPases act as binary switches by cycling between an inactive (GDP-bound) and an active (GTP-bound) state, and guanine nucleotide exchange factors (GEF) are known to play a crucial role in the activation of the small GTPases by stimulating the exchange of GDP for GTP (Rossman *et al.*, 2005).

In 2001, two research groups reported that mutations in the *ALS2* gene caused a juvenile recessive form of amyotrophic lateral sclerosis (ALS), termed ALS2 (OMIM 205100), and a rare recessive form of primary lateral sclerosis (PLSJ; OMIM 606353) (Hadano *et al.*, 2001; Yang *et al.*, 2001). The *ALS2* gene encodes a novel 184-kDa protein, termed ALS2 or alsin, comprising three predicted GEF domains, i.e., regulator of chromosome condensation (RCC1) (Ohtsubo *et al.*, 1987) -like domain (RLD) (Rosa *et al.*, 1996), the Dbl homology and pleckstrin homology (DH/PH) domains (Schmidt and Hall, 2002), and a vacuolar protein sorting 9 (VPS9) domain

METHODS IN ENZYMOLOGY, VOL. 403

0076-6879/05 $35.00
DOI: 10.1016/S0076-6879(05)03026-0

(Burd *et al.*, 1996; Horiuchi *et al.*, 1997; Kajiho *et al.*, 2003; Saito *et al.*, 2002; Tall *et al.*, 2001). In addition, eight consecutive membrane occupation and recognition nexus (MORN) motifs (Takeshima *et al.*, 2000) are noted in the region between the DH/PH and VPS9 domains (Fig. 1). Recently, we identified the ALS2-associated Rab5-specific GEF activity that is mediated by the carboxy-terminal MORN/VPS9 domain of ALS2, and have also shown that ALS2 localizes preferentially onto the early endosome compartments in neuronal cells (Otomo *et al.*, 2003). Since the family of Rab GTPases has emerged as a central player for vesicle budding, motility/trafficking, and fusion (Zerial and McBride, 2001), ALS2 may be implicated in unique vesicle/membrane dynamics in neuronal cells through the activation of Rab5. Most recently, a novel *ALS2* homologous gene, termed *ALS2CL* (ALS2 C-terminal like), has been identified (Devon *et al.*, 2005; Hadano *et al.*, 2004), and its 108-kDa protein product, ALS2CL (Fig. 1), is shown to modulate the Rab5-mediated vesicle/membrane trafficking and dynamics in the cells (Hadano *et al.*, 2004).

In this chapter, we describe methods for the purification of the newly identified members of Rab5GEF family, ALS2 and ALS2CL, as well as the small GTPase Rab5, which are utilized to conduct a number of biochemical analyses including GEF activity and *in vitro* binding assays for ALS2/ALS2CL and Rab5.

Proteins Used for *In Vitro* Functional Analyses

Purification of Recombinant ALS2 and ALS2CL Proteins

Expression Constructs. The mammalian expression constructs for the N-terminally FLAG-tagged ALS2 and ALS2CL proteins are generated as follows. FLAG-linker is generated by annealing two complementary oligonucleotides (forward: 5′-CGCGAGCCACCATGGATTACAAG-GATGACGACGATAAGACGCGTGTTAACC-3′; reverse; 5′-CCGG-

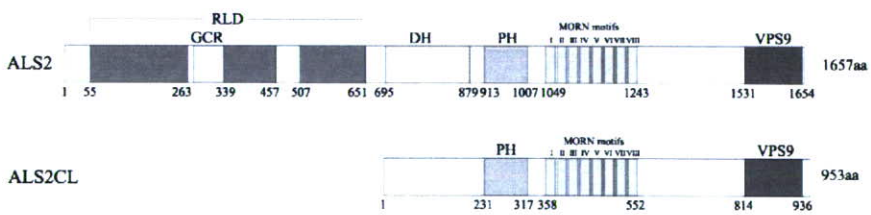

FIG. 1. Schematic representation of the domains and motifs identified in ALS2 and ALS2CL.

GGTTAACACGCGTCTTATCGTCGTCATCCTTGTAATCCATGGT-GGCT-3′), and then inserted into the *Mlu*I–*Cfr*9I sites of pCI-neo Mammalian Expression Vector (Promega), generating the pCIneoFLAG vector. The full-length cDNA fragments of the *ALS2/Als2* and *ALS2CL/Als2cl* genes are amplified by reverse transcriptase polymerase chain reaction (RT-PCR) from human or mouse brain total RNA using the following primer pairs: human *ALS2* and ALS2-L: 5′-tctcgagacgcgtATGGACT C A AAGAAGAGAA GCTCAACAGAG-3′/ALS2-R; 5′-tatgcatcccgggtCTAGTTAAGCTTCT CACGCTGAATCTGGTAG-3′; mouse *Als2* and mALS2-L: 5′-tctcga-gacgcgtATGGACTCAAAGAAGAAAAGCTCAACAG-3′/ mALS2-R; 5′-tatgcatcccgggtCTAGTTAAGCTTCTCCCGCTGAATCTGGAAG-3′; human *ALS2CL* and ALS2CL-L: 5′-atatacgcgtATGTGCAACCCTGAG-GAGGCAGC-3′/ ALS2CL-R; 5′-atatgcggccgcCTACCAGAGCTCCC TGGAGTGCC-3′; and mouse *Als2cl* and mALS2CL-L: 5′-atatacgcgtAT GTCTAGCTCTGAGGAGGCAGAC-3′/ mALS2CL-R; 5′-atatgcggccgc TCAC CAGAG-ATCTCTAGCGTCCC-3′, respectively. The resulting *ALS2/Als2* cDNAs are digested with *Mlu*I–*Cfr*9I, and inserted into the *Mlu*I–*Cfr*9I sites of the pCIneoFLAG vector, generating pCIneoFLAG-ALS2_L and pCIneoFLAG-mALS2_L. The *ALS2CL/Als2cl* cDNAs are digested with *Mlu*I–*Not*I, and inserted into the *Mlu*I–*Not*I sites of the pCIneoFLAG vector, generating pCIneoFLAG-ALS2CL and pCIneo-FALG-mALS2CL. The DNA sequences of the insert as well as the flanking regions in each clone are verified by sequencing. All other truncated mutants for ALS2 (Otomo *et al.*, 2003) described in this chapter were generated principally using the same method except for the primer pairs used.

Cell Culture and Transfection. COS-7 cells are cultured in Dulbecco's modified Eagle's medium (DMEM) supplemented with 10% heat-inactivated fetal bovine serum (Invitrogen), 100 U/ml penicillin, and 100 μg/ml streptomycin. Cells are seeded in a T150 flask at a density of 2×10^6 cells/flask and cultured for ~24 h, and then transfected with 10 μg of each plasmid construct using the Effectene Transfection Reagent (Qiagen). After 48 h of transfection, cells are harvested by centrifugation and washed twice with ice-cold PBS(-) by repeating the suspension and centrifugation at +4°. The resulting cell pellets are stably stored at −80° for at least 6 months.

Partial Purification of FLAG-Tagged ALS2/ALS2CL by Immunoprecipitation. Pellets of COS-7 cells obtained from the transfection with 10 μg of pCIneoFLAG construct/T150 flask are resuspended with 1 ml of Buffer A (50 m*M* Tris–HCl, pH 7.4, 150 m*M* NaCl, 1 m*M* EDTA, 2% [w/v] Tween-20, 1 tablet of Complete protease inhibitor cocktail [Roche]/50 ml of the buffer) and lysed for 3 h at 4° with a gentle rotation. Supernatants

are recovered by centrifugation at 12,000×*g* for 15 min at 4°, and are immediately subjected to immunoprecipitation using EZview Red ANTI-FLAG M2 Affnity Gel (Sigma). In brief, a 60-μl aliquot of the slurry of gel beads is washed with 2 × 1 ml of ice-cold Buffer A, mixed with an approximately 1 ml of the supernatant, and incubated for 16 h at 4° with a gentle rotation. The M2 affinity gel beads are then washed three times with ice-cold Buffer A. To estimate the approximate amount of conjugating FLAG-tagged ALS2/ALS2CL on the beads, appropriate amounts of the immunoprecipitates are analyzed by sodium dodecyl sulfate–polyacrylamide gel electrophoresis (SDS-PAGE) followed by either silver or Coomassie blue staining in combination with Western blotting analysis using an anti-FLAG antibody. The purity of the FLAG-tagged human ALS2 and its truncated mutants (silver staining) and FLAG-tagged human and mouse ALS2CL (Coomassie blue staining) prepared by this method is shown in Fig. 2. Finally, the amino-terminally FLAG-tagged ALS2/ALS2CL proteins bound to the M2 affinity gel beads are resuspended in appropriate volumes of GEF buffer (25 m*M* Tris–HCl, pH 7.4, 50 m*M*

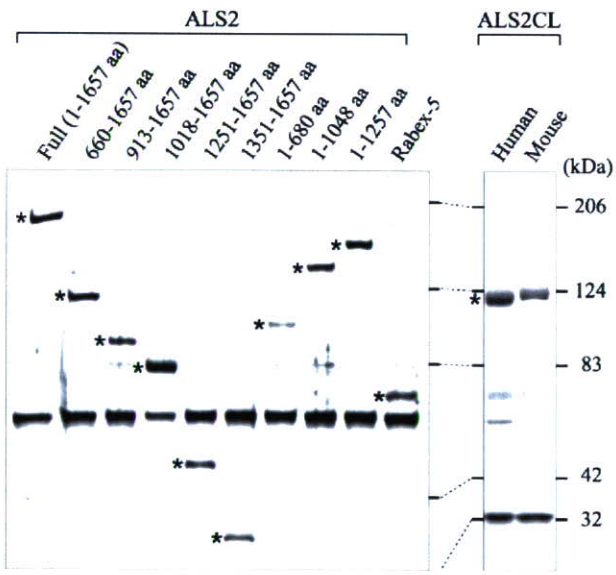

FIG. 2. SDS-PAGE analysis of the immunoprecipitated FLAG-tagged human ALS2, various truncated human ALS2 mutants, human Rabex-5 (Rab5GEF), and human and mouse ALS2CL. Asterisk indicates each immunoprecipitated protein. Left panel (ALS2, its truncated mutants, and Rabex-5), sliver staining; right panel (ALS2CL), Coomassie blue staining. Positions of size markers are shown on the right.

NaCl, 20 m*M* $MgCl_2$, 1 m*M* CHAPS) and used for GDP/GTP exchange assay *in vitro*. For longer storage, the choice of detergent in the buffer is very important. The immunoprecipitated ALS2/ALS2CL bound onto the affinity gel beads can be stored in Buffer A at 4° for at least 1 year without a significant loss of GEF activities on Rab5A. However, the buffer containing 0.1% IGEPAL CA-630 (NP-40) instead of Tween-20, for example, leads to the formation of the aggregated form of ALS2 only after several weeks, thereby decreasing their enzymatic activities.

Purification of the Recombinant Rab5A Protein

Expression Construct and Transformation. To generate the bacterial expression construct for Rab5A, the human *RAB5A* cDNA is amplified from human brain total RNA by RT-PCR, using primer pairs (Rab5A-L: 5′-atatggatccgcgaattcaATGGCTAGTCGAGGCGCAACAAGACCC-3′ and Rab5A-R: 5′-atatggatcctcgagTTAGTTACTACAACACTGATTCCTGGT TGG-3′). The amplified *RAB5A* cDNA is digested with *Bam*HI and *Xho*I and cloned into the *Bam*HI–*Xho*I sites of the pGEX-6P-2 (Amersham Pharmacia). The resulting construct, pGEX6P-Rab5A (Otomo *et al.*, 2003), is used to transform *Escherichia coli* BL21(DE3)pLysS (Novagen).

Expression and Purification of Rab5A. To express GST-fused Rab5A, 10 ml of LB medium containing 100 μg/ml of ampicillin is inoculated with a single colony of the BL21(DE3) pLysS transformant and grown to saturation overnight at 37°. Aliquots of culture (~5 ml) are then used to seed a larger culture (250 ml), and further grown at 37° until OD_{600} ~1.4. The fusion protein is induced with 0.1 m*M* isopropyl thio-β-D-galactoside (IPTG) at 18° for 3 h. Bacteria are collected by centrifugation at 5000×*g* for 15 min at 4°, and frozen at −80° until use. Bacterial pellets are resuspended in 20 ml of Bacterial Lysis buffer (50 m*M* Tris–HCl, pH 8.0, 100 m*M* NaCl, 2 m*M* EDTA, 2 m*M* dithiothreitol [DTT], 10% [v/v] glycerol, 1% [w/v] CHAPS, 1 m*M* 4-aminophenylmethanesulfonyl fluoride [p-APMSF], 0.4 mg/ml lysozyme), and incubated for 30 min on ice, followed by the gentle sonication (1 min) on ice. The lysate is centrifuged at 10,000×*g* for 30 min at 4° to remove cell debris and insoluble materials, and the cleared supernatant obtained is mixed with a 1 ml slurry of the glutathione-Sepharose 4B beads (Amersham Pharmacia), which is prewashed with PBST (PBS[-], 0.5 % [v/v] Triton X-100). After mixing them for at least 3 h (or overnight) at 4°, the beads are washed four times with 10 ml of PBST and packed into a disposable column. The column is washed with 4 × 5 ml of PBST and then with 3 ml of Bacterial Lysis buffer. GST-fused Rab5A is then eluted with 9 ml of 15 m*M* reduced glutathione in Bacterial

Lysis buffer, snap frozen with liquid nitrogen, and stored at −80° until needed.

To purify Rab5A, the GST portion of the fusion protein is removed by treatment with PreScission Protease (Amersham Pharmacia) as follows. First, to remove reduced glutathione contained in the GST-fused Rab5A sample and to replace Bacterial Lysis buffer with PSP buffer (50 m*M* Tris–HCl, pH 7, 100 m*M* NaCl, 1 m*M* EDTA, 1 m*M* DTT) appropriate for enzymatic cleavage, a 1-ml aliquot of GST-Rab5A is applied to a HiTrap Desalting column (bed volume, 5 ml, Amersham Pharmacia), which is preequilibrated with PSP buffer and eluted in 10 × 500-μl fractions of PSP buffer. Following elution, the protein concentration of each fraction is measured by a UV spectrophotometer at OD_{280} and three peak fractions are pooled (~1.5 ml). Approximately 0.5 ml of PSP buffer containing 0.04% (v/v) Triton X-100 is added to this pooled fraction (final 0.01% Triton X-100 in PSP), and the resulting fraction is subjected to the digestion with PreScission Protease (20 units) overnight at 4°. As PreScission Protease is a GST fusion protein, the cleaved GST portion of GST-Rab5A and PreScission Protease can be removed simultaneously by applying the digested samples onto a glutathione-Sepharose 4B beads column, and a follow-through fraction that contains the purified Rab5A is collected. Finally, ~2 ml of the follow-through fraction is dialyzed twice using a Slide-A-Lyzer 10k Dialysis Cassette (PIERCE) against an excess volume (2 × 1 liter) of GXP loading buffer (25 m*M* Tris–HCl, pH 7.5, 50 m*M* NaCl, 10 m*M* EDTA, 5 m*M* $MgCl_2$, 1 m*M* DTT, 1 m*M* CHAPS) overnight at 4°, and the concentration of the purified Rab5A is determined using the Bradford reaction. SDS–PAGE analysis of the expression and purification of Rab5A using the above protocol is shown in Fig. 3. Using this method, 250 ml of the starting bacterial culture is enough to obtain 1–2 mg of purified Rab5A. It is noted that although most of the other small GTPases can be purified by the same method, the yield of each small GTPase is varied.

Assays for GEF Activity

GXP Loading

The purified Rab5A (200 pmol) is loaded with [^{3}H]GDP (0.8 nmol; 370 GBq/mmol) (Amersham Pharmacia) in GXP loading buffer for 30 min at 30°. To stabilize nucleotide binding, $MgCl_2$ is added to a final concentration of 20 m*M*, and the mixture is cooled to 4°. The GDP-loaded protein sample is then applied onto the PD-10 column (Amersham Pharmacia),

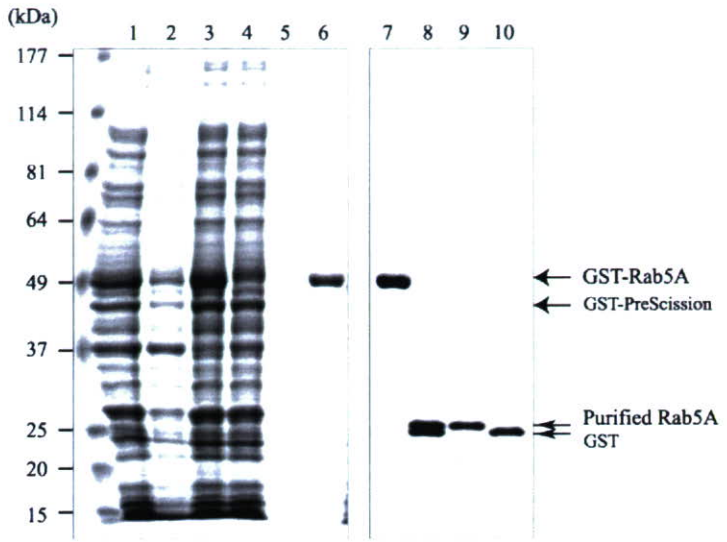

FIG. 3. Expression and purification of the recombinant Rab5A protein. Aliquots of protein sample at each purification step are analyzed by SDS-PAGE, followed by Coomassie blue staining. Lane 1, whole bacterial extract; lane 2, insoluble pellet fraction; lane 3, soluble supernatant fraction; lane 4, supernatant of soluble fraction after treatment with glutathione-Sepharose 4B beads; lane 5, proteins remaining on the beads after elution with reduced glutathione; lanes 6 and 7, eluted fraction from the beads (purified GST-Rab5A); lane 8, the digested GST-Rab5A with PreScission Protease; lane 9, the follow-through fraction (purified Rab5A); lane 10, proteins trapped onto glutathione-Sepharose 4B beads (GST and GTS-PreScission). Positions of size markers are shown on the left.

and eluted in 15 × 100 μl fractions in GEF buffer on ice. Aliquots (2.5 μl) of each fraction are counted in a liquid scintillation counter to determine the radioactivity, and six peak fractions are pooled. The loaded Rab5A is immediately used for the GDP dissociation assay, or snap frozen in liquid nitrogen and stored at −80° until needed.

GDP Dissociation Assay

Four picomoles of the [^{3}H]GDP-loaded Rab5A is preincubated for 5 min at 30°, and a nucleotide dissociation reaction was initiated by the addition of gel beads conjugating 2 pmol equivalent of the immunoprecipitated FLAG-tagged ALS2 or ALS2CL protein, and further incubated for 60 min at 30° in a final volume of 40 μl GEF buffer in the presence of 5 m*M* GTP. Reactions are then terminated by the addition of 2 ml of ice-cold

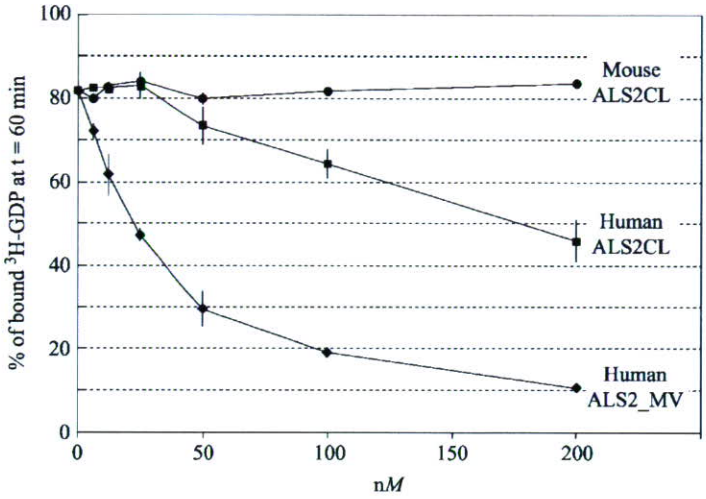

FIG. 4. The dose–response curve of the GDP dissociation activity of ALS2 and ALS2CL on Rab5A. Each value represents mean ± SD ($n = 3$) of the percentage of [^{3}H]GDP bound to Rab5A after 60 min in the presence of a given amount of either human ALS2_MV (ALS2 _1018–1657 aa) (diamonds), human ALS2CL (squares), or mouse ALS2CL (circles).

STOP buffer (25 m*M* Tris-HCl, pH 7.5, 100 m*M* NaCl, 20 m*M* $MgCl_2$) and filtered through BA85 nitrocellurose filters (Schleicher & Schell), followed by washing the filters with 20 ml of STOP buffer. The radioactivity trapped on the filters is counted by a scintillation counter, and the percentage of the dissociated [^{3}H]GDP is calculated. Typical results of the GDP dissociation assay for ALS2 and ALS2CL on Rab5A are shown in Fig. 4 and elsewhere (Hadano *et al.*, 2004; Kunita *et al.*, 2004; Otomo *et al.*, 2003).

GTP-Binding Assay

Rab5A is preloaded with 100 m*M* of either GTPγS or GDP essentially in the same manner as above. Gel beads conjugating a 2 pmol equivalent of the immunoprecipitated FLAG-tagged ALS2 and 0.5 pmol of [^{35}S] GTPγS (37 TBq/mmol; Amersham Pharmacia) are preincubated for 5 min at 30°. Reactions are initiated by the addition of 4 pmol of Rab5AGDP, Rab5AGTPγS, or nucleotide-free Rab5A, and incubated for the required time, typically for 60 min, at 30° in a final volume of 40 μl GEF buffer. Reactions are then terminated and filtered, followed by scintillation counting, as indicated above (Otomo *et al.*, 2003).

Functional Interactions of ALS2/ALS2CL

Interaction of ALS2/ALS2CL with Rab5

Purified Rab5A (4 pmol), which is preloaded with either GTPγS or GDP, or left unloaded with any nucleotides, is incubated with the FLAG-M2 affinity beads conjugating 4 pmol of the immunopurified FLAG-tagged ALS2 in 100 μl of the modified GEF buffer (25 m*M* Tris–HCl, pH 7.5, 100 m*M* NaCl, 20 m*M* $MgCl_2$, 1.5 m*M* CHAPS, 0.1% [w/v] skim milk) containing 50 μ*M* of either GTPγS or GDP, or without nucleotides, for 2 h at 30° with a gentle shaking. After washing four times with 1 ml of the same buffer without skim milk, bound Rab5A is coeluted with the FLAG-tagged ALS2 proteins by the addition of SDS–PAGE sample buffer, and each protein is detected by Western blotting analysis using anti-Rab5 or anti-FLAG-M2 antibody. Results of the *in vitro* Rab5A binding assay are shown in Fig. 5. We have also reported the interaction between ALS2CL and Rab5A (Hadano *et al.*, 2004).

Characterization of Oliogomerized ALS2 by Gel Filtration

Recently, by immunoprecipitation and gel filtration analyses, we demonstrated that ALS2 homooligomerizes in mammalian cells (Kunita *et al.*, 2004). In this chapter, a procedure for the gel filtration of the recombinant ALS2 protein is described. In brief, FLAG-tagged ALS2

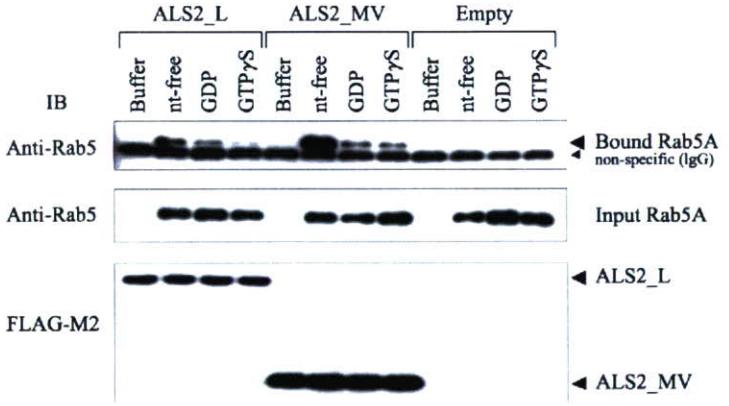

FIG. 5. *In vitro* Rab5A-binding assay. Nucleotide free (nt-free), GDP bound (GDP), or GTPγS bound (GTPγS) forms of Rab5A are incubated with the FLAG-M2 beads conjugating FLAG-tagged ALS2_L (full-length) or ALS2_1018–1657 aa (AL2_MV), or with FLAG-M2 beads alone (empty) as a control. IB, antibodies used for Western blotting analysis.

proteins on the FLAG-M2 gel beads are resuspended in Buffer B (50 m*M* Tris–HCl, pH 7.5, 150 m*M* NaCl, 0.1% IGEPAL CA-630) and subsequently eluted with Buffer B containing 500 ng/ml 3×FLAG peptide (Sigma) for 1 h at 4°. Approximately 30 pmol of FLAG-tagged ALS2 is applied to the Superdex 200 column (HR 10/30 Amersham Pharmacia), which is preequilibrated with Buffer B. Elution is carried out at 4° at a flow rate of 0.3 ml/min with a fraction volume of 0.5 ml. Fractions are subjected to Western blotting analysis with anti-ALS2 polyclonal antibody (MPF 1012–1651) (Kunita *et al.*, 2004). The elution profile of the column is calibrated with the sizing standards (Amersham Pharmacia) of thyroglobulin (669 kDa), ferritin (440 kDa), catalase (232 kDa), aldorase (158 kDa), and ovalbumin (43 kDa). Gel filtration profiles for ALS2 have been reported by Kunita (2004).

Discussion

We have described here the procedures for the purification of ALS2, ALS2CL, and Rab5A, and the GEF activity assay as well as the *in vitro* binding for ALS2 and Rab5A. Using a mammalian expression system, ALS2 is highly expressed in the detergent-soluble fraction, and thus is easily enriched and purified by immunoprecipitation. Overexpressed untagged ALS2 as well as endogenous ALS2 can also be immunoprecipitated from cultured cells and/or tissue (brain) extract using the anti-ALS2 polyclonal antibody (unpublished observations). It is noteworthy that the truncated ALS2 molecules that retain Rab5GEF activity turn to a solely insoluble feature. On the other hand, ALS2CL is mostly distributed to the detergent-insoluble fraction in the cells, and thus the amount of ALS2CL in the soluble fraction is rather small. However, the expression level of the ALS2CL construct in COS-7 cells is extremely high, so that enough protein for several biochemical assays can be obtained by immunoprecipitation. Conversely, most ALS2 truncated mutants are unstable when overexpressed in the cells (Yamanaka *et al.*, 2003) and are also insoluble in nature (unpublished observations). Therefore, to purify such proteins, a rather larger scale of culture and transfection is required when the mammalian expression system is adopted. Use of a proteasome inhibitor, such as MG132 (Calbiochem) (Yamanaka *et al.*, 2003), is also effective in increasing the yield of proteins. Alternatively, bacterial expression (Otomo *et al.*, 2003) and the baculovirus-Sf9 cell systems (Topp *et al.*, 2004) can also be used for the preparation of ALS2 fragments. In fact, we have routinely used the bacterial expression system for ALS2 proteins utilizing for the antibody generation and affinity columns. However, as the homooligomerization of ALS2 is crucial for ALS2-associated Rab5GEF activity *in vitro*

and ALS2-mediated endosome dynamics in the cells (Kunita *et al.*, 2004), a careful assessment of every experimental procedure, which may alter the properties for ALS2/ALS2CL, should be required, no matter what procedures would be used.

Acknowledgments

This work was funded by the Japan Science and Technology Agency, and in part by research grants from Research on Psychiatric and Neurological Diseases and Mental Health from the Ministry of Health, Labour and Welfare, and a Grant-in-Aide for Scientific Research from the Japan Society for the Promotion of Science.

References

Burd, C. G., Mustol, P. A., Schu, P. V., and Emr, S. D. (1996). A yeast protein related to a mammalian Ras-binding protein, Vps9p, is required for localization of vacuolar proteins. *Mol. Cell Biol.* **16,** 2369–2377.

Da Silva, J. S., and Dotti, C. G. (2002). Breaking the neuronal sphere: Regulation of the actin cytoskeleton in neuritogenesis. *Nat. Rev. Neurosci.* **3,** 694–704.

Devon, R. S., Schwab, C., Topp, J. D., Orban, P. C., Yang, Y.-Z., Pape, T. D., Helm, J. R., Davidson, T.-L., Rogers, D. A., Gros-Louis, F., Rouleau, G., Horazdovsky, B. F., Levitt, B. R., and Hayden, M. R. (2005). Cross-species characterization of the *ALS2* gene and analysis of its pattern of expression in development and adulthood. *Neuobiol. Dis.* **18,** 243–257.

Etienne-Manneville, S., and Hall, A. (2002). Rho GTPases in cell biology. *Nature* **420,** 629–635.

Govek, E.-E., Newey, S. E., and Van Aelst, L. (2005). The role of the Rho GTPases in neuronal development. *Genes Dev.* **19,** 1–49.

Hadano, S., Hand, C. K., Osuga, H., Yanagisawa, Y., Otomo, A., Devon, R. S., Miyamoto, N., Showguchi-Miyata, J., Okada, Y., Singaraja, R., Figlewicz, D. A., Kwiatkowski, T., Hosler, B. A., Sagie, T., Skaug, J., Nasir, J., Brown, R. H., Jr., Scherer, S. W., Rouleau, G. A., Hayden, M. R., and Ikeda, J.-E. (2001). A gene encoding a putative GTPase regulator is mutated in familial amyotrophic lateral sclerosis 2. *Nat. Genet.* **29,** 166–173.

Hadano, S., Otomo, A., Suzuki-Utsunomiya, K., Kunita, R., Yanagisawa, Y., Showguchi-Miyata, J., Mizumura, H., and Ikeda, J.-E. (2004). ALS2CL, the novel protein highly homologous to the carboxy-terminal half of ALS2, binds to Rab5 and modulates endosome dynamics. *FEBS Lett.* **575,** 64–70.

Horiuchi, H., Lippe, R., McBride, H. M., Rubino, M., Woodman, P., Stenmark, H., Rybin, V., Wilm, M., Ashman, K., Mann, M., and Zerial, M. (1997). A novel Rab5 GDP/GTP exchange factor complexed to Rabaptin-5 links nucleotide exchange to effector recruitment and function. *Cell* **90,** 1149–1159.

Kajiho, H., Saito, K., Tsujita, K., Kontani, K., Araki, Y., Kurosu, H., and Katada, T. (2003). RIN3: A novel Rab5 GEF interacting with amphiphysin II involved in the early endocytic pathway. *J. Cell Sci.* **116,** 4159–4168.

Kunita, R., Otomo, A., Mizumura, H., Suzuki, K., Showguchi-Miyata, J., Yanagisawa, Y., Hadano, S., and Ikeda, J.-E. (2004). Homo-oligomerization of ALS2 through its unique

carboxy-terminal region is essential for the ALS2-associated Rab5 guanine nucleotide exchange activity and its regulatory function on endosome trafficking. *J. Biol. Chem.* **279,** 38626–38635.

Luo, L. (2000). Rho GTPases in neuronal morphogenesis. *Nat. Rev. Neurosci.* **1,** 173–180.

Ohtsubo, M., Kai, R., Furuno, N., Sekiguchi, T., Sekiguchi, M., Hayashida, H., Kuma, K., Miyata, T., Fukushige, S., Murotsu, T., Matsubara, K., and Nishimoto, T. (1987). Isolation and characterization of the active cDNA of the human cell cycle gene (RCC1) involved in the regulation of onset of chromosome condensation. *Genes Dev.* **1,** 585–593.

Otomo, A., Hadano, S., Okada, T., Mizumura, H., Kunita, R., Nishijima, H., Showguchi-Miyata, J., Yanagisawa, Y., Kohiki, E., Suga, E., Yasuda, M., Osuga, H., Nishimoto, T., Naurumiya, S., and Ikeda, J.-E. (2003). ALS2, a novel guanine nucleotide exchange factor for the small GTPase Rab5, is implicated in endosomal dynamics. *Hum. Mol. Genet.* **12,** 1671–1687.

Rosa, J. L., Casaroli-Marano, R. P., Buckler, A. J., Vilaró, S., and Barbacid, M. (1996). p532, a giant protein related to the chromosome condensation regulator RCC1, stimulates guanine nucleotide exchange on ARF1 and Rab proteins. *EMBO J.* **15,** 4262–4273.

Rossman, K. L., Der, C. J., and Sondek, J. (2005). GEF means go: Turning on Rho GTPases with guanine nucleotide-exchange factors. *Nat. Rev. Mol. Cell Biol.* **6,** 167–180.

Saito, K., Murai, J., Kajiho, H., Kontani, K., Kurosu, H., and Katada, T. (2002). A novel binding protein composed of homophilic tetramer exhibits unique properties for the small GTPase Rab5. *J. Biol. Chem.* **277,** 3412–3418.

Schmidt, A., and Hall, A. (2002). Guanine nucleotide exchange factors for Rho GTPases: Turning on the switch. *Genes Dev.* **16,** 1587–1609.

Takeshima, H., Komazaki, S., Nishi, M., Iino, M., and Kangawa, K. (2000). Junctophilins: A novel family of junctional membrane complex proteins. *Mol. Cell* **6,** 11–22.

Tall, G. G., Barbieri, M. A., Stahl, P. D., and Horazdovsky, B. F. (2001). Ras-activated endocytosis is mediated by the Rab5 guanine nucleotide exchange activity of RIN1. *Dev. Cell* **1,** 73–82.

Topp, J. D., Gray, N. W., Gerard, R. D., and Horazdovsky, B. F. (2004). Alsin is a Rab5 and Rac1 guanine nucleotide exchange factor. *J. Biol. Chem.* **279,** 24612–24623.

Van Aelst, L., and Symons, M. (2002). Role of Rho family GTPases in epithelial morphogenesis. *Genes Dev.* **16,** 1032–1054.

Yamanaka, K., Vande Velde, C., Eymard-Pierre, E., Bertini, E., Boespflug-Tanguy, O., and Cleveland, D. W. (2003). Unstable mutants in the peripheral endosomal membrane component ALS2 cause early-onset motor neuron disease. *Proc. Natl. Acad. Sci. USA* **100,** 16041–16046.

Yang, Y., Hentati, A., Deng, H. X., Dabbagh, O., Sasaki, T., Hirano, M., Hung, W. Y., Ouahchi, K., Yan, J., Azim, A. C., Cole, N., Gascon, G., Yagmour, A., Ben-Hamida, M., Pericak-Vance, M., Hentati, F., and Siddique, T. (2001). The gene encoding alsin, a protein with three guanine-nucleotide exchange factor domains, is mutated in a form of recessive amyotrophic lateral sclerosis. *Nat. Genet.* **29,** 160–165.

Zerial, M., and McBride, H. (2001). Rab proteins as membrane organizers. *Nat. Rev. Mol. Cell Biol.* **2,** 107–117.

Journal of Cerebral Blood Flow & Metabolism (2005), 1–13

www.jcbfm.com

A dopamine D4 receptor antagonist attenuates ischemia-induced neuronal cell damage via upregulation of neuronal apoptosis inhibitory protein

Yoshinori Okada[1,2], Harumi Sakai[1], Eri Kohiki[3], Etsuko Suga[3], Yoshiko Yanagisawa[3], Kazunori Tanaka[1], Shinji Hadano[1,3], Hitoshi Osuga[1,3] and Joh-E Ikeda[1,3,4]

[1]*Department of Molecular Neuroscience, The Institute of Medical Sciences, Tokai University, Isehara, Kanagawa, Japan;* [2]*Laboratory for Structure and Function Research, Tokai University School of Medicine, Isehara, Kanagawa, Japan;* [3]*Solution Oriented Research for Science and Technology (SORST), Japan Science and Technology Agency (JST), Tokai University School of Medicine, Isehara, Kanagawa, Japan;* [4]*Department of Paediatrics, University of Ottawa, Ottawa, Ontario, Canada*

Neuronal apoptosis inhibitory protein (NAIP/BIRC1), the inhibitor of apoptosis protein (IAP) family member, suppresses neuronal cell death induced by a variety of insults, including cell death from ischemia and stroke. The goal of the present study was to develop an efficient method for identification of compounds with the ability to upregulate endogenous NAIP and to determine the effects on these compounds on the cellular response to ischemia. A novel NAIP-enzyme-linked immunosorbent assay (ELISA)-based *in vitro* drug-screening system is established. Use of this system identified an antagonist of dopamine D4 receptor, termed L-745,870, with a potent NAIP upregulatory effect. L-745,870-mediated NAIP upregulation in neuronal and nonneuronal cultured cells resulted in decreased vulnerability to oxidative stress-induced apoptosis. Reducing NAIP expression via RNA interference techniques resulted in prevention of L-745,870-mediated protection from oxidative stress. Further, systemic administration of L-745,870 attenuated ischemia-induced damage of the hippocampal CA1 neurons and upregulated NAIP expression in the rescued hippocampal CA1 neurons in a gerbil model. These data suggest that the NAIP upregulating compound, L-745,870, has therapeutic potential in acute ischemic disorders and that our NAIP-ELISA-based drug screening may facilitate the discovery of novel neuroprotective compounds.
Journal of Cerebral Blood Flow & Metabolism advance online publication, 23 February 2005; doi:10.1038/sj.jcbfm.9600078

Keywords: antiapoptosis; dopamine receptor antagonist; IAP; ischemia; NAIP; oxidative stress

Introduction

Several studies have demonstrated that the mechanisms of ischemia-induced neuronal cell death fall on the continuum between necrosis and apoptosis (Raghupathi *et al*, 2000; Graham and Chen, 2001). While relatively more interest has been focused on prevention of cell necrosis after ischemic insults, apoptosis, with its ordered series of events, including caspase activation (Graham and Chen, 2001) and/or the perturbation of calcium homeostasis (Love, 1999), may represent a more suitable target for modulation for the goal of preventing cell death. This may be particularly true for neuronal damage after cerebral ischemia (Nitatori *et al*, 1995).

Recent studies have demonstrated that various antiapoptotic proteins, including Bcl-2, neuronal apoptosis inhibitory protein (NAIP, also called baculoviral IAP repeat-containing 1 (BIRC1)), and X-linked inhibitor of apoptosis (XIAP), are upregulated in neurons after ischemia (Graham and Chen, 2001; Krajewski *et al*, 1995; Xu *et al*, 1997, 1999). Among these antiapoptotic proteins, NAIP, the founding member of the inhibitor of apoptosis protein (IAP) family, was identified in the course

Correspondence: Dr J-E Ikeda, Department of Molecular Neuroscience, The Institute of Medical Sciences, Tokai University, Isehara, Kanagawa 259-1193, Japan.
E-mail: jei@m.med.u-tokai.ac.jp
This work was funded by the Japan Science and Technology Agency (JST). A part of the work was supported by a Grant-in-Aid for Scientific Research on Priority(C)-Advanced Brain Science Project from the Ministry of Education, Culture, Sports, Science, and Technology of Japan.
Received 4 August 2004; revised 15 November 2004; accepted 6 December 2004

of the positional cloning of the gene responsible for spinal muscular atrophy (SMA) (Roy *et al*, 1995). In actuality, the primary genetic defect in SMA results from mutations in an adjacent gene, survival motor neurons (SMN). However, patients with the most severe form of SMA have large deletions that encompass both the *SMN* and *NAIP* genes. These data suggest that NAIP may also play a role in neuronal viability (Gavrilov *et al*, 1998; Hsieh-Li *et al*, 2000; Monani *et al*, 2000).

Indeed, overexpression of NAIP by adenovirus-mediated gene transfer reduces ischemic cell damage in the rat hippocampus (Xu *et al*, 1997). Further, ectopic NAIP expression rescues motor neurons after peripheral nerve axotomy (Perrelet *et al*, 2000) and preserves nigrostriatal dopaminergic function in the intrastriatal 6-hydroxydopamine (6-OHDA) rat model of Parkinson's disease (Crocker *et al*, 2001). Moreover, NAIP promotes motor neuron survival through the intracellular signaling of glial cell-derived neurotrophic factor (GDNF) (Perrelet *et al*, 2002). Finally, unlike other IAP proteins and Bcl-2 family proteins, NAIP exerts a unique antiapoptotic activity against oxidative stresses. These findings suggest that NAIP plays an important role in the protection of the neuronal cells from apoptotic insults, and that upregulation of endogenous NAIP may represent a therapeutic approach for prevention of oxidative stress-induced neuronal cell damage.

Therefore, the goal of the present study was to develop an efficient method for identification of compounds with the ability to upregulate endogenous NAIP and to determine the effects of these compounds on the cellular response to ischemia.

Materials and methods

Chemicals

A total of 953 compounds, including 3-[(4-[4-chlorophenyl]piperazine-1-yl)methyl]-[1H]-pyrrolo[2,3-*b*] pyridine-trihydrochloride (L-745,870) listed in 'Neurochemicals, Signal Transduction Agents, Pharmacological Probes and Biochemicals compounds; Tocris Cookson Ltd', was purchased from Tocris Cookson Ltd (Bristol, UK) and subjected to drug-screening experiments. Drug concentrations were tested in a range from 1 to 100 μmol/L. All other cytotoxins including menadione, H_2O_2, α-naphthoquinone, 2,3-dimethoxy-1,4-naphthoquinone (DMNQ), actinomycin D, staurosporine, *cis*-platinum, okadaic acid, oligomycin, and etoposide were purchased from Sigma-Aldrich (St Louis, MO, USA).

Antibodies

Two independent anti-human NAIP antibodies, IB9 and ME1, were generated. IB9, a mouse monoclonal antibody, was raised using an epitope of the human NAIP C-terminal peptide (amino acids 841 to 1052), and a polyclonal antibody, ME1 (1:3,000 dilution), was obtained by immunizing rabbits with recombinant NAIP peptide (amino acids 256 to 587). ME1 recognizes the BIR3 region of NAIP and crossreacts with the mouse and gerbil NAIP proteins (data not shown). Other antibodies used in this study included rabbit polyclonal anti-XIAP antibody (#AF822; 1:1,000; R&D Systems, Minneapolis, MN, USA), rabbit polyclonal anti-cIAP-1 antibody (#AF818; 1:1,000; R&D Systems), rabbit polyclonal anti-cIAP-2 antibody (#AF817; 1:1,000; R&D Systems), rabbit polyclonal anti-Survivin antibody (#NB500-201; 1:1,000; Novus Biologicals, Littleton, CO, USA), rabbit polyclonal anti-Bcl-2 antibody (#SC-783; 1:1,000; Santa Cruz Biotechnology, CA, USA), rabbit polyclonal anti-Bcl-xL antibody (#SC-634; 1:1,000; Santa Cruz Biotechnology), and mouse monoclonal anti-β-tubulin antibody (#SC-5274; 1:50,000; Santa Cruz Biotechnology).

Cell Lines and Culture Conditions

The human monocyte-derived cell line, THP-1, was cultured in RPMI-1640 (Invitrogen, Carlsbad, CA, USA), while HeLa and SH-SY5Y neuroblastoma cells were cultured in Dulbecco's modified Eagle's medium (DMEM) (Invitrogen). All culture media contained penicillin (50 IU/mL) and streptomycin (50 μg/mL) and were supplemented with 10% fetal calf serum. SH-SY5Y cells, which were seeded with a density of 4×10^5 cells/well in six-well plates, were differentiated by treatment with all-*trans*-retinoic acid (Tocris Cookson) at a concentration of 10 μmol/L.

NAIP-ELISA and Screening of NAIP Upregulating Compounds

NAIP-neuronal apoptosis inhibitory protein-enzyme-linked immunosorbent assay (ELISA)-based screening with THP-1 cells was conducted to identify compounds that induced endogenous NAIP expression. THP-1 cells were cultured in 24-well plates at a density of 2×10^5 cells/well for 24 h, followed by incubation in the presence of tested compounds for either 24 or 72 h. Cells were then lysed with NP40 buffer (50 mmol/L Tris-HCl, pH 7.5, 150 mmol/L NaCl, 1% NP40, and protein inhibitor cocktail (Complete; Roche Diagnostics, Indianapolis, IN, USA)). Aliquots of extracts were subjected to the NAIP-ELISA assay, with 1B9 as primary antibody conjugated to the ELISA plate and with ME1 as secondary antibody for quantification of NAIP immunoreactivity. Assays were conducted according to standard ELISA procedure (Crowther, 1995).

Western Blot Analysis

The extracts from cultured cells were electrophoretically separated on 5% to 20% SDS-polyacrylamide gels and transferred onto polyvinylidene difluoride (PVDF) membranes (Bio-Rad Laboratories, Hercules, CA, USA). Membranes were then incubated with the indicated primary antibodies in TBST buffer (50 mmol/L Tris-HCl; pH 7.4, 150 mmol/L NaCl, 0.1% (w/v) Tween-20) for 2 h, after

incubation with the peroxidase-linked secondary anti-rabbit IgG (#NA934; Amersham Pharmacia Biotech, Uppsala, Sweden) or anti-mouse IgG (#NA931; Amersham Pharmacia Biotech) antibody for 1 h. Signals were detected using ECL Plus (Amersham Pharmacia Biotech).

Cell Viability Assay

Approximately 1×10^5 cells, which were either pretreated with 10 μmol/L of L-745,870 for 24 h or left untreated, were plated on a 96-well plate and incubated for 5 h at 37°C. The appropriate amounts of the cytotoxins, including free radical generating compounds (DMNQ: 120 μmol/L, menadione: 20 to 80 μmol/L, α-naphthoquinone: 60 μmol/L and H_2O_2: 30 μmol/L), kinase inhibitor (staurosporine: 1 nmol/L), ATPase inhibitor (oligomycin: 100 μmol/L), DNA-damaging reagent (*cis*-platinum: 100 μmol/L), phosphatase inhibitor (okadaic acid: 100 nmol/L), and topoisomerase II inhibitors (actinomycin D: 1 μmol /L and etoposide: 100 μmol/L), were added, and the preparation was allowed to incubate for another 1 to 10 h. The medium was then replaced with fresh medium containing 10% (v/v) alamarBlue (AccuMed International, Westlake, OH, USA), followed by incubation for an additional 4 h at 37°C. Cell numbers were counted fluorometrically as per the alamarBlue Assay instructions.

Flow-Cytometric Analysis of Apoptotic/Necrotic Cell Death

Quantification of the apoptotic/necrotic cell death was performed by flow cytometry in conjunction with the MEBCYTO Apoptosis Kit (MBL, Nagoya, Japan). In brief, HeLa cells that were pretreated with or without L-745,870 were plated on a six-well plate (3×10^5 cells/well). After 4 h of incubation, menadione (or H_2O_2) was added to the cells, followed by incubation for an additional 4 h (or 40 mins for H_2O_2). The cells were washed once with phosphate-buffered saline (PBS) and suspended in fresh medium for Annexin V-FITC and propidium iodide (PI) labeling, which was performed according to the manufacturer's instructions (MBL). The cells were sorted and analyzed by FACScan (Beckton Dickinson, San Jose, CA, USA). Cell damage was classified according to the extent of staining of AnnexinV-FITC and PI (Quadrant analysis). Quadrants were comprised of the upper left (UL; AnnexinV−/PI+), upper right (UR; AnnexinV+/PI+), low left (LL; AnnexinV−/PI−), and low right (LR; AnnexinV+/PI−). LL, LR, and UR represent the cells in normal state, early stage of apoptosis, and late stage of apoptosis/necrosis, respectively.

RNA Interference

Neuronal apoptosis inhibitory protein RNA interference (RNAi) was achieved by expressing the hairpin-forming short RNA molecules generated from a portion of the 3′UTR of the human *NAIP/BIRC1* gene. Briefly, 19-nucleotide-long inverted repeats, 5′-GTCAACTCCCCT-CCCCTTG-3′ (sense) and 5′-CAAGGGGAGGGGAGTT-GAC-3′ (antisense), which were intervened with the 9-nucleotide spacer (TTCAAGAGA), were inserted downstream of the U6 promoter of pSilencer 1.0-U6 vector (Ambion, Austin, TX, USA), generating pSilencer 1.0-U6-NAIP. HeLa cells, which were either pretreated with L-745,870 for 24 h or left untreated, were cotransfected with 10 μg of pSilencer 1.0-U6-NAIP and 1 μg of pMACS K^k.II (Miltenyi Biotec, Bergisch Gladbach, Germany) using FuGENE6 (Roche Diagnostics). After 48 h, the transfected cells were magnetically enriched and cultured for 24 h. NAIP expression and cell viability were analyzed by Western blotting and by the alamarBlue Assay, respectively.

Generation of Forebrain Ischemic Model in Gerbils

All animal experimental procedures were performed in accordance with the guidelines of the Tokai University School of Medicine Committee on Animal Care and Use. Twelve-week-old Male Mongolian gerbils (Clea Japan Inc., Tokyo, Japan), weighing 70 to 80 g, were used. Animals were anesthetized with halothane (4%) in a mixture of N_2O/O_2 (70:30) initially, and halothane was gradually decreased to 2% for maintenance of anesthesia during surgery. Under anesthesia, a femoral artery catheter was placed to monitor mean arterial blood pressure, and rectal and temporal muscle temperatures were monitored and maintained at 37°C±0.5°C via a heating pad and radiant heat during and after surgery. Forebrain ischemia was induced by bilateral common carotid artery occlusion (BCCAO) using 3-mm sugita-aneurysm clips (Kirino and Sano, 1984). After 10 mins of occlusion, the aneurysmal clips were removed to allow reperfusion, and complete reperfusion of the arteries was verified by direct visual observation. Sham-operated gerbils underwent identical surgery with the exception of the BCCAO procedure. Under these experimental conditions, in which a relatively severe ischemic condition was used, all animals survived until fixation.

To investigate the *in vivo* effect of L-745,870 (Tocris Cookson Ltd) on ischemia-induced cell death, the compound was dissolved in physiologic saline and was administered to gerbils at a dose of 7 mg/kg ($n=6$), 70 mg/kg ($n=7$), 140 mg/kg ($n=7$), or 210 mg/kg ($n=6$). We have administered the compound to the animals 1 h before ischemic surgery to ensure the protection of neurons from the oxidative stress-induced cell death. This experimental protocol was designed based on the *in vitro* experimental data in which the pretreatment with the compound effectively protects cultured cells from the menadione-induced insults (refer to Figures 1 to 4). Administration of the compound was performed intragastrically via oral cannula under anesthesia. Vehicle-treated animals ($n=7$) received physiologic saline alone. Sham-operated animals ($n=3$) were administered with a compound dose of 210 mg/kg.

Measurement of Regional Cerebral Blood Flow

To analyze the effect of the compound on regional cerebral blood flow (CBF), a subset of animals underwent measure-

ment of CBF at 2 and 24 h after administration of L-745,870 (210 mg/kg) or vehicle. Cerebral blood flow was measured by the hydrogen clearance method via a platinum wire electrode stereotaxically inserted into the right hippocampus using coordinates of 2 mm posterior and 2 mm lateral to the bregma, and 2.5 mm below the brain surface in a flat cranial presentation, as previously reported (Osuga *et al*, 2000).

Histopathology

After 3 days of reperfusion, animals were anesthetized with 4% halothane and perfused with 60 mL of 4% paraformaldehyde in phosphate buffer (pH 7.4) via a catheter placed in the heart. The brains were removed, fixed in 10% formalin for 10 days, and embedded in paraffin. Paraffin sections were sliced at a thickness of 7 μm for histopathologic and immunohistochemical evaluation. Neuronal cell density of the CA1 subfield of the hippocampus, that is, the number of intact CA1 pyramidal neurons per 1 mm linear length of pyramidal cell layer, was measured by counting 7 μm sections stained with hematoxylin and eosin from 3 to 7 independent animals in a double-masked manner.

Immunohistochemistry

Brain sections were subjected to NAIP and XIAP immunohistochemistry with polyclonal anti-human NAIP (ME1) and XIAP antibodies (R&D Systems Inc.), respectively, and stained using the Vectastain elite ABC kit (Vector Laboratories Inc., Burlingame, CA, USA) according to the manufacturer's instructions. In brief, after deparaffinization, the sections were washed with 0.01 mol/L PBS (pH 7.2) for 5 mins and were incubated with anti-NAIP (5 μg/mL) or anti-XIAP (5 μg/mL) antibody overnight at 4°C. The sections were rinsed three times with PBS containing 0.05% Triton X-100 for 10 mins, incubated with biotinylated secondary antibody for 3 h, and then incubated with avidin–biotin–peroxidase complex for 1 h at room temperature. Finally, the sections were treated with 0.5% 3,3′-diaminogenzidine (DAB) and 0.01% H_2O_2 in Tris-HCl buffer (pH 7.5), and the DAB reaction products were observed under a microscope.

Statistical Analysis

All data in this study are presented as mean $\pm$ s.e. Data were analyzed for significance using Student's *t*-test for pair-wised comparisons or ANOVA followed by Scheffe's test for multiple comparisons between groups (Statview 5.0 software; SAS, Cary, NC, USA). A *P*-value <0.05 was considered as reaching statistical significance.

Results

Identification of NAIP Upregulating Compounds

To identify compounds with the ability to induce NAIP expression, 953 compounds (Tocris) were screened using NAIP-ELISA. Compounds were arbitrarily categorized as 'downregulator' ($n=16$) if the resulting NAIP level was less than 70% of the normal endogenous level (i.e., $\sim$12 ng/mL), or 'upregulator' ($n=30$) if the resulting NAIP level was more than 200% of the normal endogenous NAIP level (Table 1).

To examine whether the 30 identified NAIP upregulators suppressed menadione-induced cell death, THP-1 cell viability assays were performed in cells pretreated with menadione followed by the addition of each NAIP upregulator. All 30 compounds exerted a protective effect against menadione-induced cell death with variable degrees (Table 1). The compound that exerted the most potent protective effect was L-745,870, a dopamine D4 receptor antagonist (Figure 1A). This compound was used for subsequent experiments.

L-745,870 Protects a Variety of Cultured-Cells Against Menadione-Induced Cell Death

To determine whether the protective effect of L-745,870 on THP-1 cells was specific to cell type, cell viability studies were also conducted in HeLa and SH-SY5Y (differentiated neuroblastoma by all-*trans*-retinoic acid treatment) cells after exposure to the compound. L-745,870 protected both cell lines from menadione-induced cell death (Figures 1A, THP-1; B, HeLa; and C, SH-SY5Y). Further, the dose-

Table 1 Screening of 953 Tocris compounds by NAIP-ELISA, and viability assays after challenging with menadione-induced oxidative stress in THP-1 cells

NAIP level	*NAIP concentration*			*Cell viability (%)*
	Mean $\pm$ s.e. (ng/mL)	*Minimum (ng/mL)*	*Maximum (ng/mL)*	*(n) (menadione; 40 μmol/L)*
Untreated (control)	12.4 $\pm$ 0.3 (240)	11.8	12.7	31–37% (30)
Compound treated				
Unchanged	12.9 $\pm$ 0.4 (907)	10.1	21.3	ND*
Upregulator	54.8 $\pm$ 12.1 (30)	31.8	78.8	45–93% (30)
Downregulator	8.6 $\pm$ 0.8 (16)	7.1	9.1	ND*

NAIP, neuronal apoptosis inhibitory protein; ELISA, enzyme-linked immunosorbent assay; *ND, not determined. Number in each parenthesis indicates the number of tested compounds.